11-27-2018

An Electron-Rich Calix[4]arene-Based Receptor with Unprecedented Binding Affinity for Nitric Oxide

Denan Wang
Marquette University, denan.wang@marquette.edu

Lena V. Ivanova
Marquette University

Maxim V. Ivanov
Marquette University

Saber Mirzaei
Marquette University

Qadir K. Timerghazin
Marquette University, qadir.timerghazin@marquette.edu

See next page for additional authors

Chemistry : A European Journal, Vol. 24, No. 66 (November 27, 2018): 17439-17443. DOI.

An Electron-Rich Calix[4]arene-Based Receptor with Unprecedented Binding Affinity for Nitric Oxide

Denan Wang
Department of Chemistry, Marquette University, Milwaukee, Wisconsin
Lena V. Ivanova
Department of Chemistry, Marquette University, Milwaukee, Wisconsin
Maxim V. Ivanov
Department of Chemistry, Marquette University, Milwaukee, Wisconsin
Saber Mirzaei
Department of Chemistry, Marquette University, Milwaukee, Wisconsin
Qadir K. Timerghazin
Department of Chemistry, Marquette University, Milwaukee, Wisconsin
Scott A. Reid
Department of Chemistry, Marquette University, Milwaukee, Wisconsin

Rajendra Rathore
Department of Chemistry, Marquette University, Milwaukee, Wisconsin

Abstract

Calixarenes have found widespread application as building blocks for the design and synthesis of functional materials in host–guest chemistry. The ongoing desire to develop a detailed understanding of the nature of NO bonding to multichromophoric π-stacked assemblies led us to develop an electron-rich methoxy derivative of calix[4]arene (**3**), which we show exists as a single conformer in solution at ambient temperature. Here, we examine the redox properties of this derivative, generate its cation radical ($\mathbf{3}^{+\cdot}$) using robust chemical oxidants, and determine the relative efficacy of its NO binding in comparison with model calixarenes. We find that $\mathbf{3}/\mathbf{3}^{+\cdot}$ is a remarkable receptor for NO^+/NO, with unprecedented binding efficacy. The availability of precise experimental structures of this calixarene derivative and its NO complex, obtained by X-ray crystallography, is critically important both for developing novel functional NO biosensors, and understanding the role of stacked aromatic donors in efficient NO binding, which may have relevance to biological NO transport.

Calixarenes derived from base-catalyzed condensation of 4-*tert*-butylphenol/formaldehyde have found widespread application as building blocks for the design and synthesis of functional materials in host–guest chemistry.[1-7] Such calixarenes exist as multiple conformers, affording further tailoring of their properties. It has been shown that, upon its activation via 1−e^- oxidation, the conformationally mobile *p-tert*-butylcalix[4]arene-OMe (**1**) binds nitric oxide (NO) with nanomolar efficiency (K>5×10^8) leading to the formation of the [**1**, $NO]^+$ complex.[8] The same complex was also obtained by mixing neutral calixarene **1** with nitrosonium cation NO^+. With the aid of X-ray crystallography, it was demonstrated that at least three (i.e., cone, paco, and 1,3-alt, see Figure 1) of the four conformers of **1** and its conformationally rigid *p-tert*-butylcalix[4]arene-OPr (**2**) analog effectively trap a single molecule of NO between a pair of cofacially arranged benzenoid rings (Figure 1). Although *p-tert*-butylcalix[4]arene-OMe (**1**) and its conformationally frozen derivatives (**2**) have been extensively explored,[8-10] they possess relatively high oxidation potentials (E_{ox1}≈1.0 V vs. Fc/Fc^+) and their cation radicals are relatively unstable.

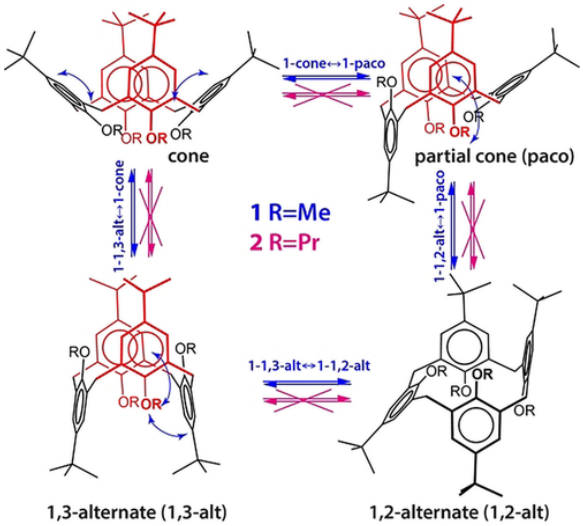

Figure 1. Four interconverting conformations of 4-*tert*-butylcalix[4]arene methyl ethers (**1**) and their rigidification in the corresponding propyl ethers (**2**). The cofacially arrayed phenyl rings marked in red provide surfaces for binding NO.

The continued interest in the role of cofacially-assembled multichromophoric aromatic systems in stabilizing NO complexes[11-17] stems from the importance of NO as a cellular messenger and the need to understand mechanisms of its intercellular migration,[18, 19] mediated possibly by assemblies of multiple aromatic residues (Figure 2 A). The desire to develop a more detailed understanding of the nature of NO bonding to multichromophoric cofacial assemblies led us to examine an electron-rich derivative of **1** (i.e., **3**, Figure 2 B), which can be prepared in a single-step synthesis from the acid-catalyzed reaction between resorcinol methyl ether (1,3,5-trimethoxybenzene) and paraformaldehyde.[20, 21]

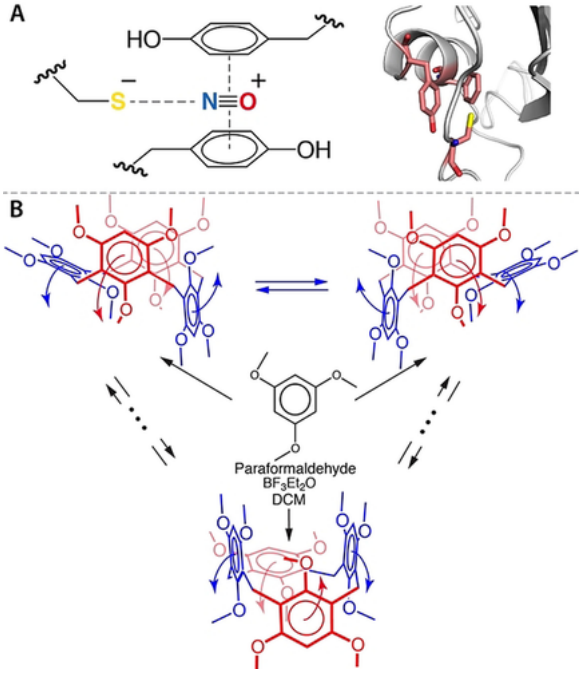

Figure 2. (A) Schematic representation of a hypothetical NO^+ stabilization by neighboring aromatic residues upon (de)-S-nitrosation and a representative example of a protein structure (PDB code: 1a44) showing cysteine residue (C132) between two aromatic tyrosine (Y157) and phenylalanine (F153) residues. (B) Synthetic scheme for the preparation of **3** and representative interconverting structures of **3**-paco (see Figure S2 in the Supporting Information for all eight structures).

Unlike **1**, where all four possible conformations are present in solution at ambient temperature,[22, 23] the methoxy-rich calixarene derivative **3** exists only as the paco conformation (Figure 2 B), with eight identical interconverting structures. The activation barrier of their interconversion is relatively small (E_a=14.6 kcal mol^{-1}), and can be frozen at ≈−20 °C.[21] Moreover, it is expected that oxidative activation of the electron-rich calixarene **3**, necessary for NO binding, can be achieved at a lower oxidation potential, owing to the presence of multiple electron-donating methoxy groups, which should add to the stability of its cation radical and, in turn, make **3** a potential candidate for NO sensing applications.

Accordingly, here we report a careful evaluation of the redox properties of **3**, generation of its cation radical using robust chemical oxidants, and determination of the relative efficacy of its NO binding in comparison with $\mathbf{1}^{+\cdot}$ and $\mathbf{2}^{+\cdot}$-paco. Aided by electrochemistry, optical, NMR, and EPR spectroscopy, X-ray crystallography, and DFT calculations, we reveal that $\mathbf{3}^{+\cdot}$ is indeed a remarkably efficient receptor for NO, with unprecedented binding efficiency. Furthermore, the availability of precise experimental structures of **3**/[**3**, NO]$^+$ obtained by X-ray crystallography is critically important not only for developing novel functional NO biosensors, but also for understanding the role of cofacially arrayed aromatic donors in efficient NO binding that may be relevant to biological NO transport. The details of these preliminary findings are described herein.

A previously reported synthesis[20] of **3** employed reaction conditions where a mixture of 1,3,5-trimethoxybenzene and equimolar paraformaldehyde in CH_2Cl_2 containing 10 % by volume trifluoroacetic acid was refluxed for 2 h, affording **3** in ≈40 % yield. By employing a catalytic amount of methanesulfonic acid and stirring the reaction mixture at ≈0 °C overnight, we obtained purer samples of **3** in improved yield (>75 %); see the Supporting Information for full experimental details and complete characterization data.

The redox potential of **3** was evaluated by electrochemical oxidation at a platinum electrode as a 2 mM solution in dichloromethane containing 0.1 M nBu$_4$N$^+$PF$_6^-$ as the supporting electrolyte, with ferrocene as added internal standard at −30 °C. Figure 3 compares the reversible cyclic voltammogram (CV) of **3**, with multiple redox waves [$E_{ox1,2}$ (**3**)=0.53, 0.66 V vs. Fc/Fc$^+$] with those of **1** and **2**-paco [E_{ox1}(**1** and **2**-paco)=0.99 V vs. Fc/Fc$^+$]. The presence of eight additional methoxy groups in **3** lowers its first oxidation by 0.46 V compared to either **1** or **2**-paco.

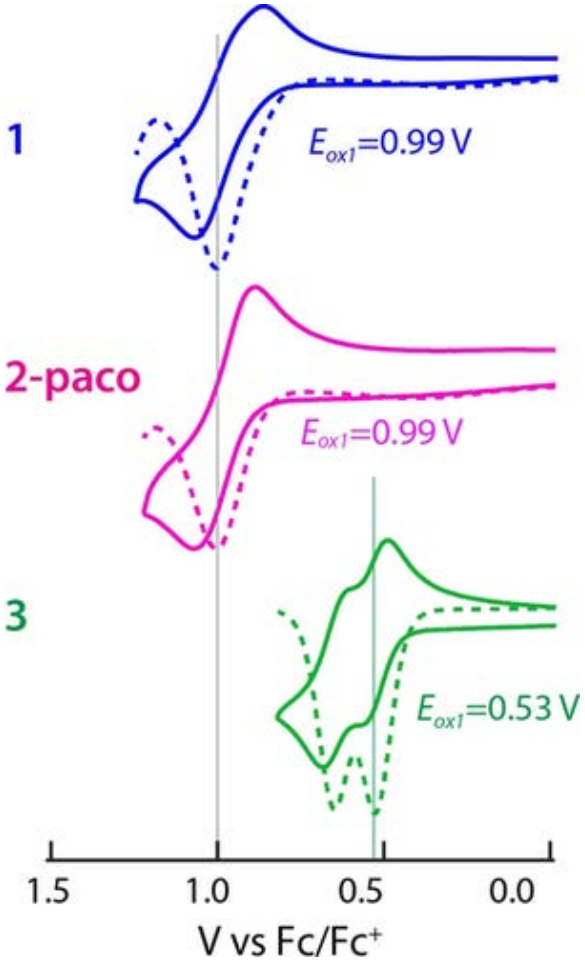

Figure 3. Cyclic voltammograms (CVs, solid lines) and overlaid square waves (SW, dashed lines) of 2 mM **1**, **2**-paco and **3** in CH_2Cl_2 (0.1 M nBu$_4$NPF$_6$) at a scan rate of 100 mV s^{-1} at −30 °C.

The cation radical of **3** was generated in solution by means of quantitative[24, 25] redox titrations using [**THEO**$^{+\cdot}$SbCl$_6^-$] (**THEO**=1,2,3,4,5,6,7,8-octahydro-9,10-dimethoxy-1,4:5,8-dimethano-anthracene, E_{red}=0.67 V vs. Fc/Fc$^+$, λ_{max}=518 nm, ϵ_{max}=7300 cm^{-1} M^{-1})[26, 27] as oxidant. For example, Figure 4 A shows the electronic spectra obtained upon an incremental (sub-stoichiometric) addition of a CH_2Cl_2 solution of **3** to a solution of [**THEO**$^{+\cdot}$SbCl$_6^-$] at −30 °C. A complete consumption of the oxidant (i.e., **THEO**$^{+\cdot}$) after the addition of 1 equiv of neutral **3**, was determined by a quantitative deconvolution[24, 25] of the component spectra of various species present at each titration point. A plot of the mole fractions of **THEO**$^{+\cdot}$ and **3**$^{+\cdot}$ against the added equivalents of **3** established a 1:1 stoichiometry of the redox reaction, that is, **3**+**THEO**$^{+\cdot}$→**3**$^{+\cdot}$+**THEO** (Figure 4 B).

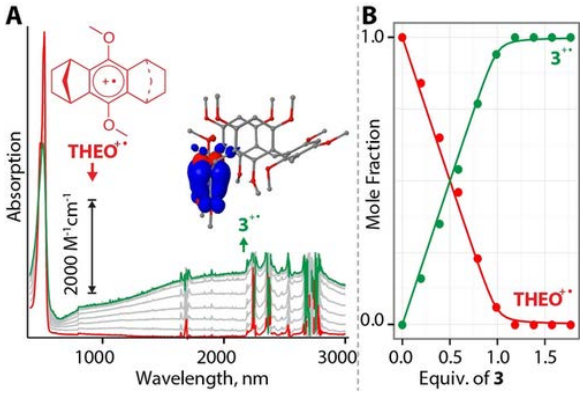

Figure 4. **A**: Spectral changes observed upon the reduction of 0.087 mM **THEO**$^{+\cdot}$ in CH_2Cl_2 (3 mL) of 2.5 mM solution of **3** in CH_2Cl_2 at −30 °C. Inset: the isovalue plot of spin density distribution in **3**$^{+\cdot}$ calculated at B1LYP-40/6-31G(d) level of theory.[28, 29] **B**: Plot of the mole fractions of **THEO**$^{+\cdot}$ (red) and **3**$^{+\cdot}$ (green) against added equivalents of neutral **3**. Symbols represent experimental points, whereas the solid lines show best-fit to experimental points using $\Delta G = E_{ox}(\mathbf{3}) - E_{red}(\mathbf{THEO}^{+\cdot}) = -150$ mV.[24]

Exposure of the generated cation radical **3**$^{+\cdot}$ to gaseous nitric oxide for 5 s leads to a dark-purple solution (see left scheme in Figure 5). The same purple color solution, assigned to the [**3**, NO]$^+$ complex, is also obtained by mixing neutral calixarene **3** with 1 equiv of oxidized nitric oxide [$NO^+SbCl_6^-$] in CH_2Cl_2 (see central scheme in Figure 5). The electronic absorption spectrum of [**3**, NO]$^+$ contains two bands at 690 and 510 nm (center spectrum of Figure 5), with the position of the latter band being similar to that of [**1**, NO]$^+$ and [**2**, NO]$^+$ at 556–572 nm (spectra on the right in Figure 5). Importantly, the [**3**, NO]$^+$ complex can also be obtained by addition of 1 equiv of **3** to the solution of [**1**, NO]$^+$ or [**2**, NO]$^+$ (right scheme in Figure 5), suggesting that the NO binding constant of **3** is at least a factor of 2400 larger than **1** or **2** (previously estimated to be $>5\times10^8$ M^{-1});[8] see details in the Supporting Information. The resulting binding constant of more than 10^{12} is unprecedented and is the largest among all known NO complexes.

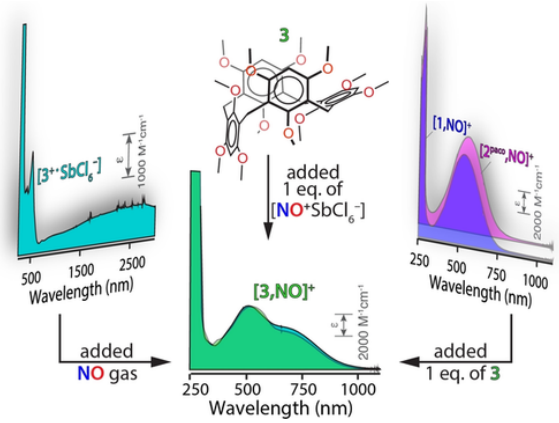

Figure 5. Electronic absorption spectra of **3**$^{+\cdot}$ (left spectrum) and [**3**, NO]$^+$ (central spectrum) obtained from addition of NO gas to **3**$^{+\cdot}$ (left scheme), by addition of [$NO^+SbCl_6^-$] to **3** (central scheme) and by addition of **3** to [**1**, NO]$^+$ and [**2**, NO]$^+$ (right scheme).

The ^{1}H-NMR spectrum of **3** shows three resolved peaks in the aromatic region arising from the protons of benzenoid rings **B** and **D** (i.e., H_B and H_D at 6.31 and 6.26 ppm, respectively) and two symmetrically equivalent protons at rings **A** and **C** ($H_{A,C}$ at 5.88 ppm), consistent with a partial cone conformation (Figure 6). Indeed, DFT calculations of NMR shifts[30] have shown that **3**-paco is the lowest-energy conformer and accounts for 98 % of the total population (Table S3 in the Supporting Information). Upon NO binding, chemical shifts of H_B and

H_D remain nearly invariant, whereas the $H_{A,C}$ peak position shifts downfield by 0.4 ppm, suggesting a significant involvement of rings **A** and **C** in NO binding.

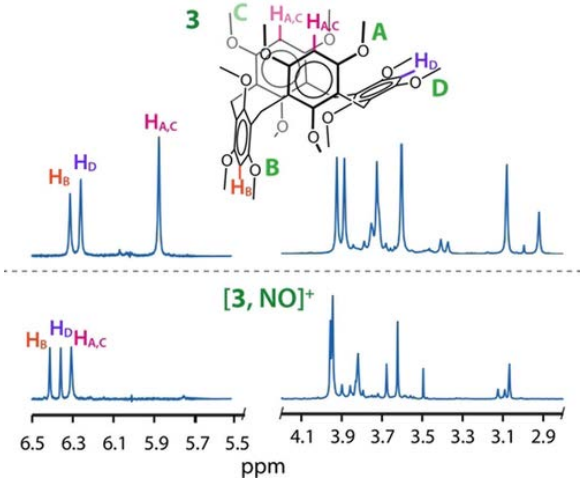

Figure 6. The ^{1}H-NMR spectra of **3** and [**3**, NO]$^+$ recorded in $CDCl_3$ at −30 °C. See proton assignment from DFT calculations (Figure S8) and variable temperature ^{1}H-NMR of **3** and [**3**, NO]$^+$ in the Supporting Information (Figure S1).

It is well known that oxidized nitric oxide, that is, [$NO^+SbCl_6^-$], is a powerful oxidant and can generate cation radicals of various aromatic electron donors. In order to probe the oxidation state of **3** in its NO complex we next obtained the EPR spectra of $\mathbf{3}^{+\cdot}$ and [**3**, NO]$^+$ (Figure 7). The EPR experiment was carried out at 77 K and a frequency of 9.62 GHz. The EPR spectrum of $\mathbf{3}^{+\cdot}$ (expectedly) showed that $\mathbf{3}^{+\cdot}$ is a cation radical with *g* value of 2.0012 (magnetic field *B*=343.5 mT). In contrast, our data showed that its NO complex is EPR silent, suggesting that [**3**, NO]$^+$ complex is bound via multiple cation-π interactions between aromatic moieties of neutral **3** and NO^+.

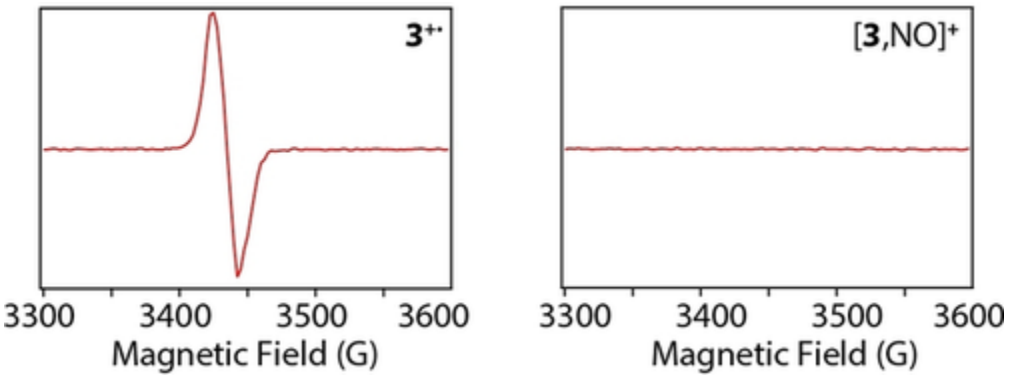

Figure 7. EPR spectra of 0.95 mM $\mathbf{3}^{+\cdot}$ and 0.99 mM [**3**, NO]$^+$ in CH_2Cl_2.

In order to probe the role of binding with NO^+ on the structure of calixarene **3**, we resorted to X-ray crystallography. Single crystals of [**3**, NO]$^+SbCl_6^-$, suitable for X-ray crystallography, were obtained by a slow diffusion of hexane into a dichloromethane solution of [**3**, NO]$^+$ held at −30 °C during the course of two days. The crystallographic analysis of the dark purple crystals of [**3**, NO]$^+$ revealed that **3** persists as a partial cone conformation in the complex (Figure 8 A). Specifically, a single molecule of NO is completely sandwiched between two aromatic rings (units **A** and **C**) inside the cavity of the calixarene (Figure 8 B) with almost no contact with the aromatic ring of unit **B**, and a partial contact with the aromatic ring of unit **D** (Figure 8 C). The distance between NO and aromatic rings **A** and **C** is substantially shorter than the van der Waals contact (2.7 vs. 3.2 Å), suggesting a strong noncovalent interaction of nitric oxide with the π-core. Indeed, comparison of the

crystal structures of [**3**, NO]$^+$ and **3** revealed that, upon NO binding, the **A**–**C** subunit distance was shortened by 0.4 Å (from 5.8 to 5.4 Å, Figure 8 D). Furthermore, the binding of NO induced appreciable bond-length changes (≤1.6 pm) in units **A** and **C**. In contrast, unit **B** remained nearly unchanged, whereas unit **D** underwent the largest bond length changes (≤2.3 pm), and the interplanar angle between **B** and **D** decreased from 69° to 64°.

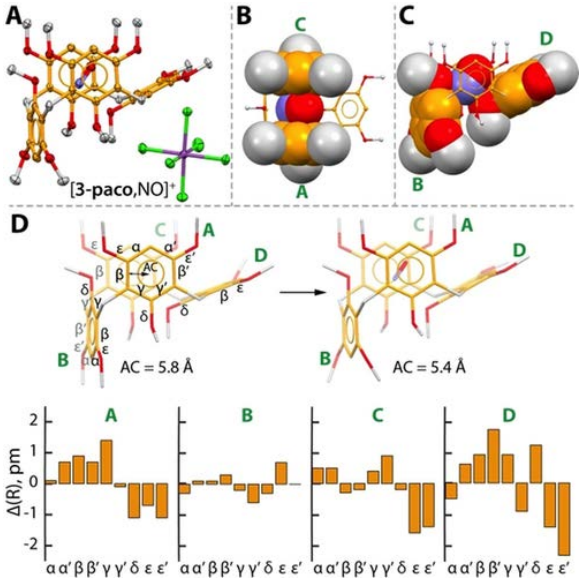

Figure 8. (A) The ORTEP diagram of [**3**, NO]$^+$$SbCl_6^-$ and its spacefilling representations illustrating a cavity formed by two sandwiched units **A** and **C** (B) and units **B** and **D** (C). (D) Capped stick representation of crystal structures of **3** and [**3**, NO]$^+$ with the bar plot representation of the bond length changes induced by NO binding.

We further emphasize that NO^+ is a powerful oxidant capable to generate cation radicals of various aromatic electron donors (Ar),[31] yet calixarene **3** forms a stable [**3**, NO]$^+$ complex despite its low oxidation potential [E_{ox1} (**3**)=0.53 V vs. Fc/Fc$^+$]. Importantly, a variety of other mono- and polyaromatic electron donors can also form stable complexes with NO^+ at ambient conditions.[8, 11-13] It has been established that, as the free energy of electron transfer (i.e., $\Delta G_{ET}=E_{ox}[Ar]-E_{red}[NO^+]$) increases, the binding energy/constant of the formation of NO complex [i.e., ΔG_{NO} K^{-1}, Eq. 1] increases.[13] For example, with the strong aromatic donor hexamethylbenzene (**HMB**), formation of the NO complex occurs with a binding constant $K=3.1\times10^4$ (Figure 9).[32]

$$NO^+ + Ar \overset{K}{\leftrightarrows} [NO, Ar]^+ \quad (1)$$

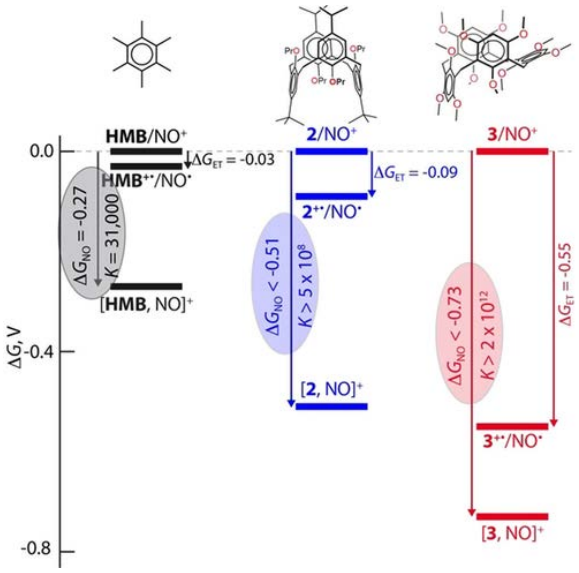

Figure 9. Energy diagram showing the interplay between binding energy of NO complex with **HMB**, **2**, and **3** (ΔG_{NO}) and electron transfer (ΔG_{ET}) between Ar and NO^+. The binding constant (K) of **3** was approximated as at least a factor of 1000 larger than **1** or **2** (previously estimated to be $>5\times10^8$ M^{-1}).[8]

It is noteworthy that although calixarene **2** has ΔG_{ET} nearly identical to that of **HMB** (−0.09 vs. −0.03 V, respectively), its NO binding constant is a factor of four larger (Figure 9). As the NO in [**2**, NO]$^+$ is sandwiched between two aromatic moieties, the binding constant suggests that the efficacy of the NO binding scales with the number of aromatic moieties involved in the NO binding, possibly due to the involvement of multiple cation-π interactions between aromatic moieties of neutral **3** and NO^+. In this context, X-ray crystallography revealed that three out of four aromatic moieties in the calixarene **3** are involved in the interaction with NO, contributing to the unprecedentedly high NO binding constant (Figure 8).

To conclude, we have demonstrated that the methoxy substituted calixarene derivative **3** is an effective receptor for NO with unprecedented binding efficiency—the largest binding constant among all known NO complexes. Furthermore, availability of the precise experimental structures of **3**/[**3**, NO]$^+$ as elucidated by electrochemistry, spectroscopy, and X-ray crystallography shed light on the origins of such binding, which lies in (1) the remarkably low oxidation potential of **3** due to the presence of 12 electron-rich methoxy groups and (2) stability of the partial cone conformation of **3** that allows stabilization of NO by three aromatic moieties. The findings of this work will advance the development of novel supramolecular hosts based on calixarenes, resorcarenes,[33, 34] etc., and lay the groundwork for the rational design of novel functional NO biosensors as well as for understanding the role of cofacially arrayed aromatic donors in efficient NO binding that may be relevant to biological NO transport.

Acknowledgements

We thank the NSF (CHE-1508677) and NIH (R01-HL112639-04) for financial support. We acknowledge the valuable assistance of Prof. Brian Bennett (MU Physics) in the EPR measurements, which were obtained on an instrument supported by an NSF MRI award (NSF CHE-1532168). We also thank Prof. Marat Talipov (New Mexico State University) for helpful discussions. Calculations were performed on the high-performance computing cluster Père at Marquette University and XSEDE.

Conflict of interest

The authors declare no conflict of interest.

References

1 S. E. Matthews, P. Schmitt, V. Felix, M. G. B. Drew, P. D. Beer, *J. Am. Chem. Soc.* 2002, **124**, 1341– 1353.

2 H. J. Kim, M. H. Lee, L. Mutihac, J. Vicens, J. S. Kim, *Chem. Soc. Rev.* 2012, **41**, 1173– 1190.

3 B. S. Creaven, D. F. Donlon, J. McGinley, *Coord. Chem. Rev.* 2009, **253**, 893– 962.

4 J. P. Chinta, B. Ramanujam, C. P. Rao, *Coord. Chem. Rev.* 2012, **256**, 2762– 2794.

5 A. Mattiuzzi, I. Jabin, C. Mangeney, C. Roux, O. Reinaud, L. Santos, J.-F. Bergamini, P. Hapiot, C. Lagrost, *Nat. Commun.* 2012, **3**, 1130.

6 F. De Riccardis, I. Izzo, D. Montesarchio, P. Tecilla, *Acc. Chem. Res.* 2013, **46**, 2781– 2790.

7 M. M. Naseer, M. Ahmed, S. Hameed, *Chem. Biol. Drug Des.* 2017, **89**, 243– 256.

8 R. Rathore, S. V. Lindeman, K. S. Rao, D. Sun, J. K. Kochi, *Angew. Chem. Int. Ed.* 2000, **39**, 2123– 2127; *Angew. Chem.* 2000, **112**, 2207– 2211.

9 Calixarene **3** is easily accessible instead of the classic *p-tert*-butyl calixarene, which requires a rather involved two-step procedure: i. the base-catalyzed condensation and polymerization of phenol and formaldehyde at high temperature; ii. pyrolysis of the precursor polymer with diphenyl ether at high temperature, followed by multiple recrystallizations from different solvents.

10 R. Rathore, S. H. Abdelwahed, I. A. Guzei, *J. Am. Chem. Soc.* 2004, **126**, 13582– 13583.

11 R. Rathore, S. V. Lindeman, J. K. Kochi, *Angew. Chem. Int. Ed.* 1998, **37**, 1585– 1587; *Angew. Chem.* 1998, **110**, 1665– 1667.

12 R. Rathore, J. K. Kochi, *J. Org. Chem.* 1998, **63**, 8630– 8631.

13 S. V. Rosokha, S. V. Lindeman, R. Rathore, J. K. Kochi, *J. Org. Chem.* 2003, **68**, 3947– 3957.

14 N. Tuteja, M. Chandra, R. Tuteja, M. K. Misra, *J. Biomed. Biotechnol.* 2004, **2004**, 227– 237.

15 D. D. Thomas, L. A. Ridnour, J. S. Isenberg, W. Flores-Santana, C. H. Switzer, S. Donzelli, P. Hussain, C. Vecoli, N. Paolocci, S. Ambs, C. A. Colton, C. C. Harris, D. D. Roberts, D. A. Wink, *Free. Radic. Biol. Med.* 2008, **45**, 18– 31.

16 T. A. Heinrich, R. S. da Silva, K. M. Miranda, C. H. Switzer, D. A. Wink, J. M. Fukuto, *Br. J. Pharmacol.* 2013, **169**, 1417– 1429.

17 L. Serre, B. Vallée, N. Bureaud, F. Schoentgen, C. Zelwer, *Structure* 1998, **6**, 1255– 1265.

18 J. O. Lundberg, M. T. Gladwin, E. Weitzberg, *Nat. Rev. Drug Discovery* 2015, **14**, 623– 641.

19 S. Pfeiffer, B. Mayer, B. Hemmens, *Angew. Chem. Int. Ed.* 1999, **38**, 1714– 1731;*Angew. Chem.* 1999, **111**, 1824– 1844.

20 T. Boinski, A. Cieszkowski, B. Rosa, A. Szumna, *J. Org. Chem.* 2015, **80**, 3488– 3495.

21 T. Ogoshi, K. Kitajima, K. Umeda, S. Hiramitsu, S. Kanai, S. Fujinami, T.-A. Yamagishi, Y. Nakamoto, *Tetrahedron* 2009, **65**, 10644– 10649.

22 Thereby attesting to a small energy difference amongst them (in the range of 2–3 kcal mol^{-1}).

23 J. Blixt, C. Detellier, *J. Am. Chem. Soc.* 1994, **116**, 11957– 11960.

24 M. R. Talipov, A. Boddeda, M. M. Hossain, R. Rathore, *J. Phys. Org. Chem.* 2016, **29**, 227– 233.

25 M. R. Talipov, M. M. Hossain, A. Boddeda, K. Thakur, R. Rathore, *Org. Biomol. Chem.* 2016, **14**, 2961– 2968.

26 R. Rathore, J. K. Kochi, *J. Org. Chem.* 1995, **60**, 4399– 4411.

27 R. Rathore, C. L. Burns, M. I. Deselnicu, *Org. Synth.* 2005, **82**, 1– 9.

28 M. V. Ivanov, M. R. Talipov, T. S. Navale, R. Rathore, *J. Phys. Chem. C* 2018, **122**, 2539– 2545.

29 M. R. Talipov, A. Boddeda, Q. K. Timerghazin, R. Rathore, *J. Phys. Chem. C* 2014, **118**, 21400– 21408.

30 R. Ditchfield, *Mol. Phys.* 1974, **27**, 789– 807.

31 M. R. Talipov, R. Rathore, *Robust Aromatic Cation Radicals as Redox Tunable Oxidants, in Organic Redox Systems: Synthesis Properties, and Applications*, Wiley, Hoboken, NJ, pp. 131, **2015**.

32 K. Lee, D. Kuchynka, J. Kochi, *Inorg. Chem.* 1990, **29**, 4196– 4204.

33 F. Ghirga, I. D'Acquarica, G. D. Monache, L. Mannina, C. Molinaro, L. Nevola, A. P. Sobolev, M. Pierini, B. Botta, *J. Org. Chem.* 2013, **78**, 6935– 6946.

34 B. Botta, I. D'Acquarica, G. D. Monache, L. Nevola, D. Tullo, F. Ugozzoli, M. Pierini, *J. Am. Chem. Soc.* 2007, **129**, 11202– 11212.

Supporting Information

As a service to our authors and readers, this journal provides supporting information supplied by the authors. Such materials are peer reviewed and may be re-organized for online delivery, but are not copy-edited or typeset. Technical support issues arising from supporting information (other than missing files) should be addressed to the authors.

Filename	Description
chem201804245-sup-0001-misc_information.pdf2.4 MB	Supplementary